Electroless Deposition of Na-Doped Iridium Oxide for Bio-Electrode Application

Wei-Ju Chao (趙偉如)[1], Kuang-Chih Tso (左貺之)[1], Yi-Chieh Hsieh (謝禕倢)[1], Tzu-Ying Chan (詹子瑩)[1]
Tzu-Ling Fan (范慈翎)[1], Jyh-Fu Lee (李志甫)[2], Chih-Wen Pao (包志文)[2] and Pu-Wei Wu (吳樸偉)[1]

[1]Department of Materials Science and Engineering, National Chiao Tung University, Hsinchu, Taiwan
[2]National Synchrotron Radiation Research Center, Hsinchu, Taiwan
ppwu@mail.nctu.edu.tw

Abstract

The implantation of bioelectronic devices is considered to be an effective approach to remedy diseases caused by neuronal disorders such as macular degeneration and Parkinson's disease. In a typical implantable biomedical device, the bio-stimulating electrode is a critical component responsible for the detection and stimulation of neuronal activities. Among many possible materials explored, the iridium oxide has attracted considerable attention for its unique electrochemical activities and biocompatibility. In this study, we have developed a wet chemical formula to fabricate Na-doped iridium oxide thin film atop a conductive ITO substrate. The as-deposited film thickness and bio-stimulating characteristics are readily controlled and the process could be implemented on a variety of substrates. Comprehensive material characterization is carried out using SEM, XAS, and XRD.

Keywords: bio-stimulating electrode, electroless deposition, Na-doped iridium oxide, XAS.

Introduction

Earlier, iridium oxide was studied intensively in applications including electrochromic devices, pseudocapacitors, and water electrolysis. With the increasing interest of implantable electronic devices, the iridium oxide has been explored as a bio-electrode because it demonstrates a significantly improved charge storage capacity over those of conventional bio-electrodes such as Pt and Pt alloys [1]. For bio-electrode consideration, a larger charge storage capacity indicates the electrode material could be physically smaller and operated at a subdued voltage. These merits become especially critical in the design of future bioelectronic devices with multielectrode arrays because each individual electrode is expected to stimulate a single neuron.

In this research, we demonstrated a wet chemical route in which the Na-doped iridium oxide was successfully deposited via a simple immersion step, which avoided typical concerns of poor adhesion and shape control associated with the predominant sputtering process. The Na-doped iridium oxide film revealed a larger charge storage capacity (CSC) as compared to that of sputtered iridium oxide due to its multiple oxidation states for additional chemical storage. In addition, the as-deposited iridium oxide passed the biocompatibility evaluation (ISO-10993) from our previous work and its application as a bioelectrode is promising [2].

Experimental

The synthesis of Na-doped iridium oxide film was conducted by an electroless deposition bath in which an aqueous solution containing 3.4 mM potassium hexachloroiridate (III) (Alfar Aesar), 3.4 mM sodium potassium tartrate (SHIMADA), 0.1 M sodium hydroxide (SHOWA), and 0.4 M sodium hypochlorite (12 wt%, SHOWA) was prepared. The entire deposition step was performed at 25℃ for 2h. Afterward, an annealing step was engaged at 450℃ in air for 2 h to improve the crystallinity of iridium oxide thin film.

Results & discussion

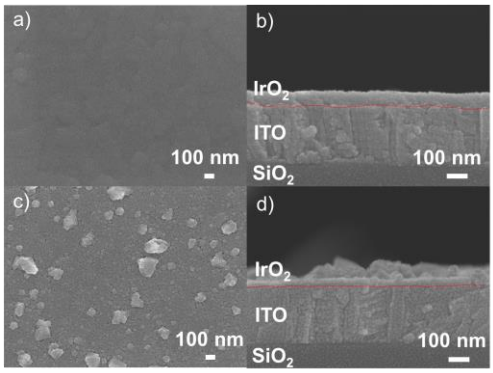

Fig. 1. The SEM images for as-deposited Na-doped iridium oxide thin film in a) top and b) cross-sectional view, as well as annealed iridium oxide thin film in c) top and d) cross-sectional view.

The SEM images for as-deposited and annealed Na-doped IrO_x thin films are displayed in Fig. 1. As shown in Fig. 1a, the top-view image for as-deposited sample exhibited a smooth and uniform surface morphology without noticeable nanoparticles from homogeneous precipitation. A similar morphology was observed for cross-sectional view shown in Fig. 1b. Fig. 1c displays the top-view image for annealed thin film, revealing numerous nanoparticles in irregular shape and their average sizes were around 141 nm. A consistent morphology was recorded for the cross-sectional view shown in Fig. 1d.

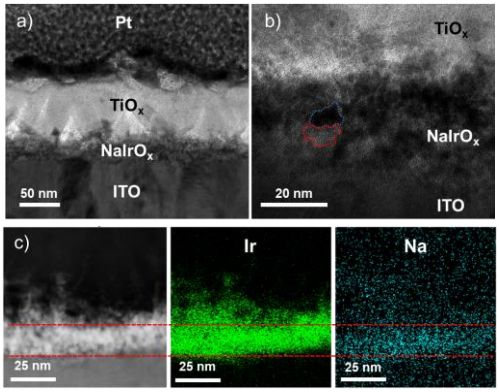

Fig. 2. The TEM images for a) annealed Na-doped iridium oxide film with TiO_x and Pt serving as the protection layer. b) A high magnification view of a). c) The TEM image for the area under EDS mapping of Ir and Na.

Fig. 2 displays the TEM/EDS images showing that the sodium was uniformly distributed in the as-deposited film.

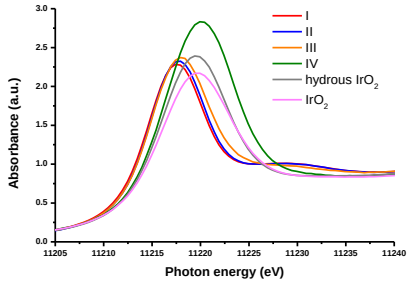

Fig. 3. The Ir L_3-edge XANES profiles for chemical bath in four distinct stages; I: aqueous K_3IrCl_6 solution, II: aqueous K_3IrCl_6 solution with $KNaC_4H_4O_6$, III: aqueous K_3IrCl_6 solution with $KNaC_4H_4O_6$ and NaOH, and IV: aqueous K_3IrCl_6 solution with $KNaC_4H_4O_6$, NaOH, and NaClO. Also shown are pristine IrO_2 and hydrous IrO_2 for comparison purpose.

To understand the deposition mechanism responsible for film growth, we employed the XAS to elucidate the valence state of iridium and its local structure in the chemical bath. Fig. 3 displays the Ir L_3-edge XAS profiles for samples in stage I, II, III, and IV, as well as standard materials including pristine IrO_2 and hydrous IrO_2 for comparison purpose. As shown in Fig 3, the oxidation states for Ir ions at stage I, II, and III were lower than that of standard hydrous IrO_2 and pristine IrO_2, indicating that their oxidation states were smaller than 4+. Since the sample in stage I was essentially Ir^{3+}, therefore, its absorption energy was adopted as the indicator for Ir^{3+}. For samples in stage II and III, their absorption energy was slightly shifted to larger energy, suggesting the Ir ions became oxidized moderately caused by the replacement of Cl^- ligands by sodium potassium tartrate and hydroxide, respectively. After the oxidant NaClO was added at stage IV, the XAS profile was significantly shifted to higher energy as compared to that of standard hydrous IrO_2 and standard IrO_2. This suggested that the oxidation state for Ir ions at stage IV was greater than 4+.

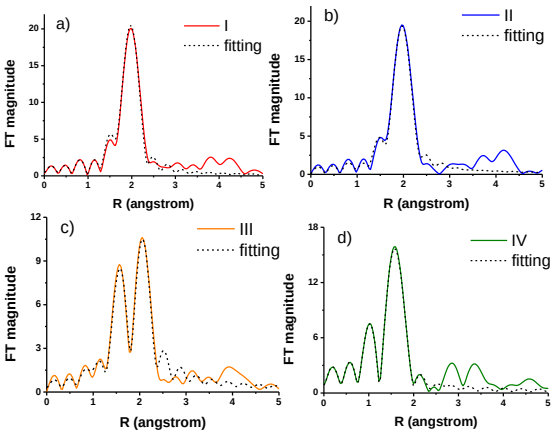

Fig. 4. The k^3-weighted Fourier-transformed EXAFS profiles and their respective fitting results for the chemical bath in four distinct stages; a) I, b) II, c) III, and d) IV.

The EXAFS fitting result from Fig. 4 indicates that the iridium local structure is undergoing a series of formation of species including $Ir^{III}(OH)Cl_5^{3-}$, $Ir^{III}(H_2O)(tartate)Cl_4^{3}$ $Ir^{III}(H_2O)(tartrate)(OH)_2Cl_2^{3-}$, and $Ir^{V}O(OH)_5^{2-}$ for stage I, II, III, and IV, respectively. At last stage, the Ir^V oxide was heterogeneously-deposited on the ITO substrate.

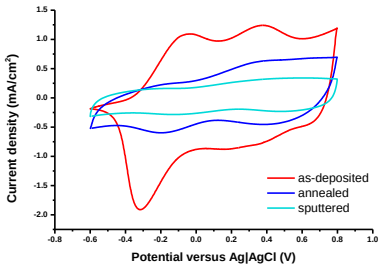

Fig. 5. The CV profiles for as-deposited and annealed Na-doped iridium oxide thin films, as well as sputtered-derived iridium oxide thin film.

In CV profiles shown in Fig. 5, the Na-doped iridium oxide thin film exhibited a larger CSC than that of sputtered-derived counterpart. However, the CSC for annealed Na-doped iridium oxide thin film was significantly smaller from that of as-deposited one. We surmised that the annulation of electroactive sites during the annealing process was responsible for the reduction in CSC.

Conclusion

In this study, we successfully fabricated the Na-doped iridium oxide thin film on an ITO substrate using a wet chemical process. By the use of XANES/EXAFS, we investigated the depositon mechanism occurring in the chemical bath. The CSC of Na-doped iridium oxide thin film was also evaluated, and it demonstated a larger charge storage capacity over conventional sputter-derived counterpart.

References

[1] S. F. Cogan, "Neural stimulation and recording electrodes", *Annual Review of Biomedical Engineering* (2008) 275-309.

[2] J. Y. Chen, Y. M. Chen, Y. Sun, J. F. Lee, S. Y. Chen, P. C. Chen, P. W. Wu, "Chemical bath deposition of IrO_2 films on ITO substrate", *Ceramics International* (2014) 14983-14990.